

Photoinduced Radical Borylation of Robust Carbon–Heteroatom Bonds

Ya-Ming Tian,^{+a} Xiang Pu,^{+a, b} Alejandro Heredero Sánchez,^{+a} Wagner Silva,^a Ruth M. Gschwind,^a and Burkhard König^{a,*}

^a Faculty of Chemistry and Pharmacy, Institute of Organic Chemistry, University of Regensburg, 93040 Regensburg, Germany
E-mail: Burkhard.Koenig@chemie.uni-regensburg.de

^b The PET/CT Center, Department of Nuclear Medicine, Sichuan Cancer Hospital and Institute, Sichuan Cancer Center, School of Medicine, University of Electronic Science and Technology of China, 610041 Chengdu, Sichuan, People's Republic of China

⁺ These authors contributed equally to this work.

Manuscript received: May 10, 2024; Revised manuscript received: September 9, 2024;

Version of record online: ■■, ■■■



Supporting information for this article is available on the WWW under <https://doi.org/10.1002/adsc.202400547>

Abstract: Photoinduced borylation has emerged as a valuable strategy for synthesizing arylboronic esters. However, photochemical transformations involving inert bonds such as C(*sp*²)–F bonds are still challenging. Herein, we report a straightforward and operationally simple method for the activation of various inert carbon–heteroatom bonds, enabling the synthesis of diverse arylboronic esters without the need for transition metals or catalysts. Mechanistic investigations reveal that the deprotonation of DMSO plays a pivotal role in the reaction, and the excited DMSO anion can undergo electron transfer to the aryl substrates activated by anionic *sp*²–*sp*³ diboron compounds, i.e., [FB₂pin₂][−], thereby facilitating the cleavage of carbon–heteroatom bonds. The reaction allows the conversion of diverse C_{aryl}–hetero bonds in batch and flow reactors into the corresponding arylboronic esters. The products can be used in a subsequent Suzuki–Miyaura cross-coupling without isolation.

Keywords: Borylation; Photochemistry; Inert carbon–heteroatom bonds; DMSO anion; Transition-metal-free

Introduction

Arylboronic esters are versatile building blocks in contemporary organic synthesis for the construction of complex molecules with use in materials science, agrochemicals, or as pharmaceuticals.^[1–14] Therefore, different methods for the synthesis of arylboronate esters have been developed. The classical approach is the reaction of trialkyl borates with lithium or magnesium aryls, followed by subsequent transesterification or hydrolysis.^[15,16] However, this requires protection and deprotection procedures. The activation of C_{aryl}–hetero bonds may be advantageous, as it selectively introduces the boron moiety to the reaction site of C_{aryl}–hetero bonds.^[17–46] However, the majority of reports have focused on the borylation of relatively weak C_{aryl}–hetero bonds, such as C(*sp*²)–I and C(*sp*²)–Br bonds, with fewer studies addressing the borylation of strong C_{aryl}–hetero bonds, such as C-

(*sp*²)–F and C(*sp*²)–O bonds. Furthermore, the thermal borylation of inert C_{aryl}–hetero bonds typically requires transition metals or harsh reaction conditions.

Photoinduced borylation is becoming a more important approach for the synthesis of arylboronate esters.^[47–84] Electronically excited molecules enable the generation of highly reactive intermediates under irradiation, thereby facilitating chemical transformations that are challenging or even unattainable through conventional thermal processes. Transition metal photocatalysis, organic photoredox catalysis, and direct photoactivation of reactants, driven by single-electron transfer processes, triplet energy transfer processes, and other radical processes, have been reported for the borylation of carbon–heteroatom bonds.^[47,66] Still, the alignment of redox potentials or energy levels of a photocatalyst with the target molecules, and the precise matching of the photon energies with the electronic transitions of the reactant molecules, impose restric-

tions on the light-mediated synthesis of organoboron compounds.^[47] Therefore, the photochemical borylation of relatively inert chemical bonds, such as the C(*sp*²)-F bond, characterized by high bond dissociation energy and high reduction potentials, remains a formidable challenge. The use of a high-energy light source (Scheme 1A), the use of transition metals (Scheme 1B and C), and the often required addition of agents (Scheme 1D) in the sparsely reported C-F borylation reactions^[62–65] pose limitations to the practical application of the reaction. Thus, a straightforward and versatile strategy for the light-induced activation and borylation of comparatively robust aryl-heteroatom bonds is desirable.

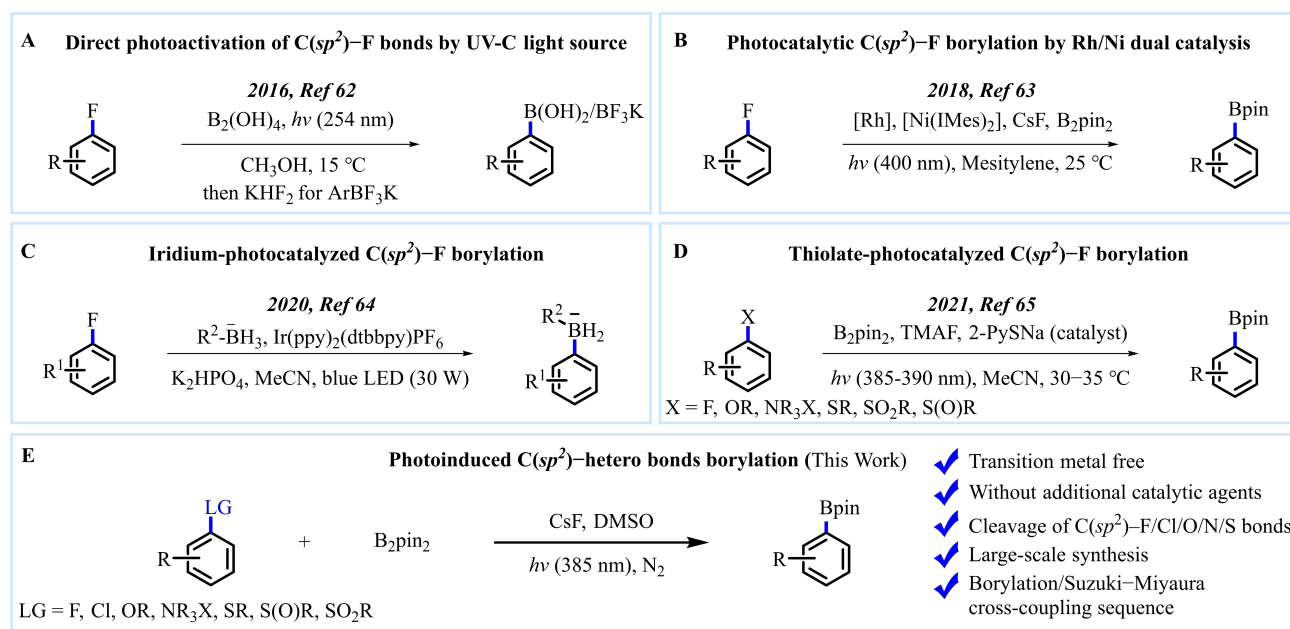
As readily available and easily handled diboron reagents, anionic *sp*²-*sp*³ diboron compounds can be synthesized through the reaction of relatively mild bases with alkoxyborate compounds.^[48,50,85,86] These anionic diboron compounds facilitate the transmetalation process in transition-metal-catalyzed borylation reactions and serve as relatively potent nucleophilic agents to expedite transition-metal-free borylation processes.^[48,50,85,86] We herein report the formation of an anionic *sp*²-*sp*³ diboron compound [FB₂pin₂]⁻, which is capable of activating aryl compounds containing inert chemical bonds. The activated aryl compounds are subsequently reduced by photoexcited DMSO anionic species, enabling the realization of borylation processes under simplified conditions without the need for transition metals or additional agents

(Scheme 1E). Employing DMSO as the solvent, bis(pinacolato)diboron (B₂pin₂) as the boron source, and CsF as the base, the system efficiently activates C(*sp*²)-F, C(*sp*²)-Cl, C(*sp*²)-O, C(*sp*²)-N, and C(*sp*²)-S bonds under light irradiation, facilitating the selective construction of aryl boronates. This method offers a versatile borylation strategy for the photo-induced activation of robust carbon-heteroatom bonds. Furthermore, it enables borylation and subsequent Suzuki-Miyaura cross-coupling reactions.

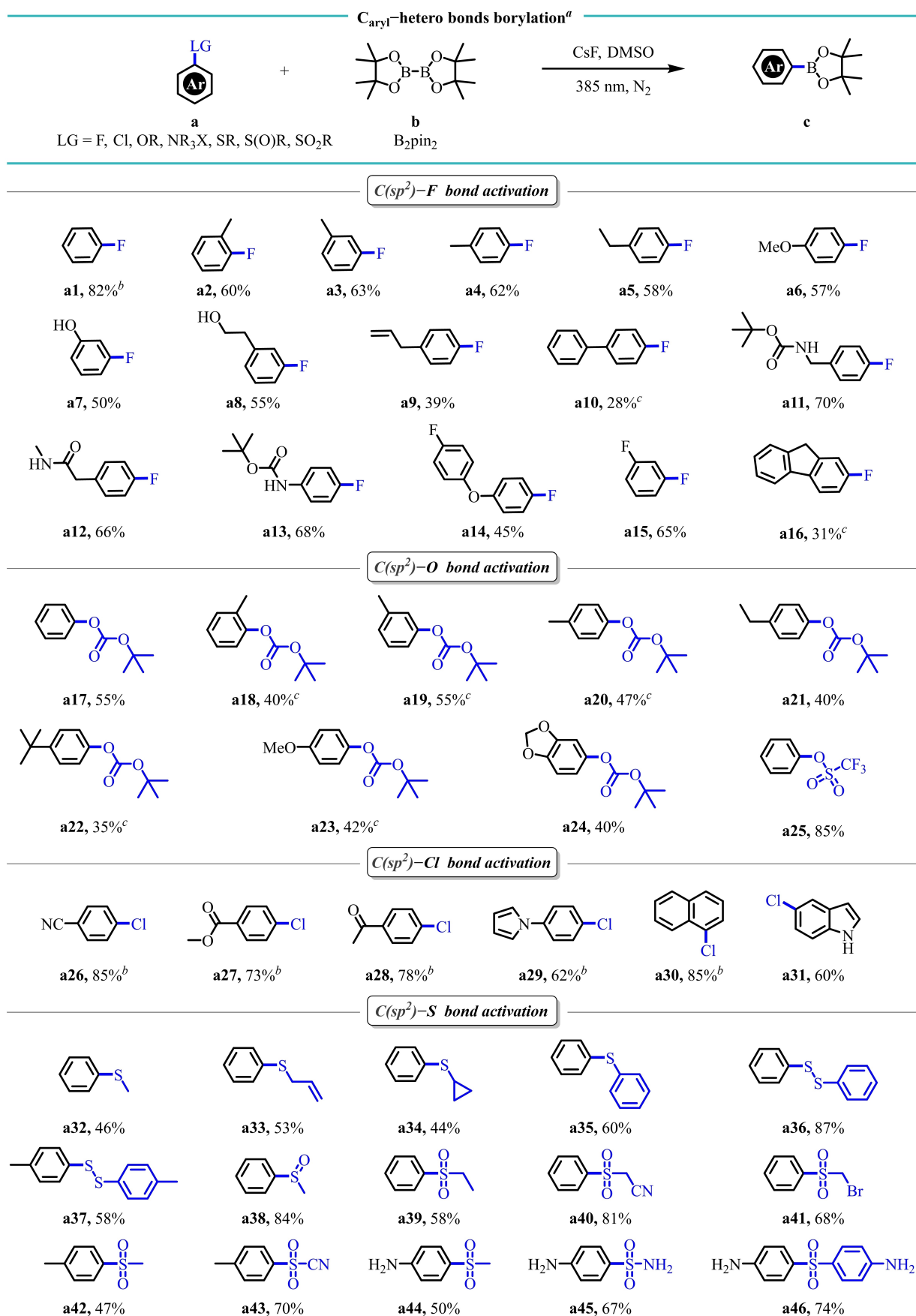
Results and Discussion

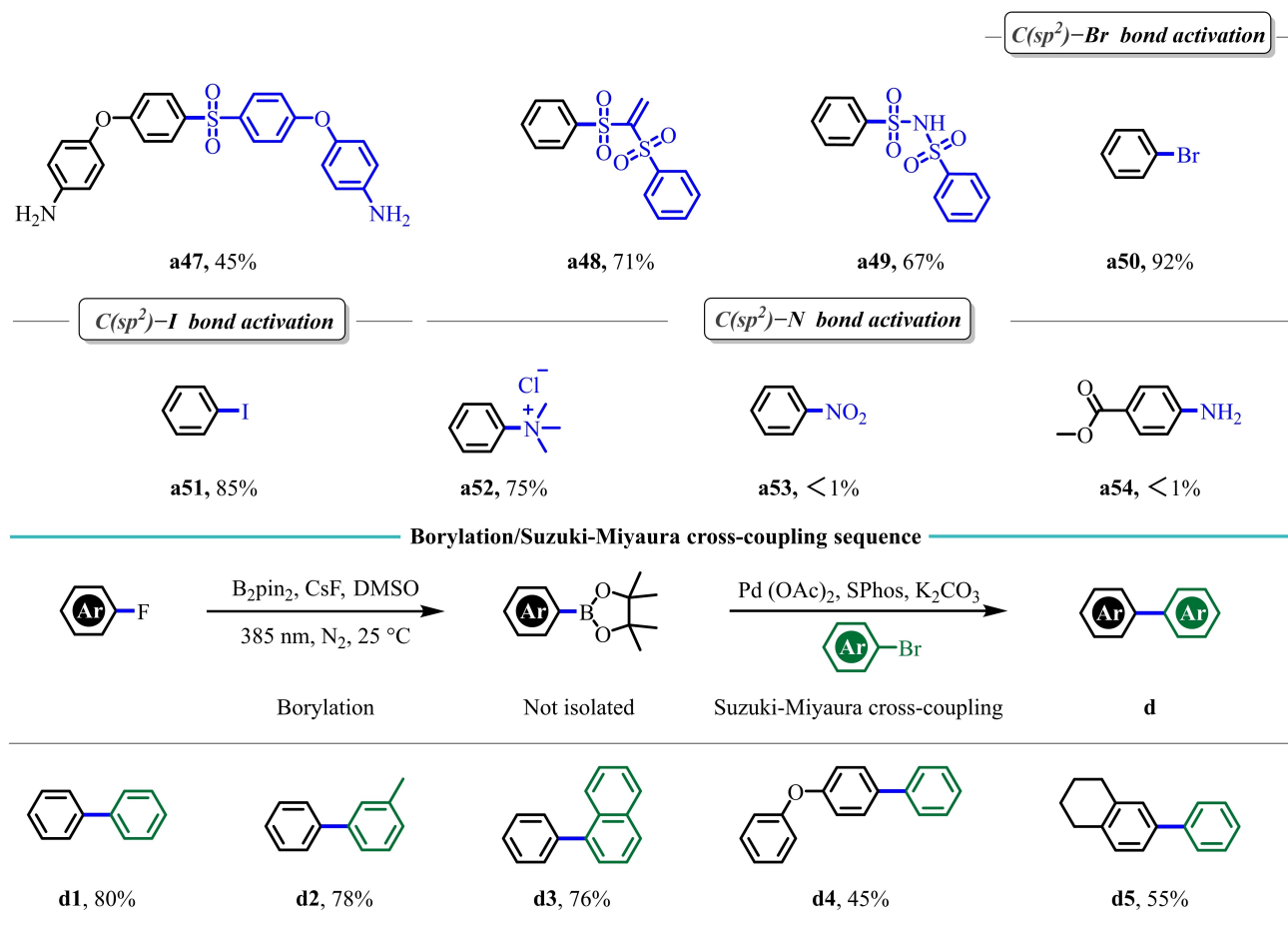
Reaction Optimization and Synthesis

We initiated our investigation for fluorobenzene (**a1**) activation by employing B₂pin₂ (**b1**) as the boron source (Tables 1 and S1). After screening different solvents and bases (Tables 1, S2 and S3), it was evident that DMSO and CsF exhibited the best performance, leading to the production of the target arylboronate compound **c1** with a yield of 90%. No product was detected without the addition of CsF confirming the crucial role of the base in the reaction (Table 1, entry 2). When the reaction was carried out at 25 °C or 60 °C under dark conditions (Table 1, entries 3 and 4), no reaction occurred, ruling out the possibility of a thermal pathway. The reaction was almost completely inhibited when exposed to air (Table 1, entry 5). Additionally, the introduction of water greatly



Scheme 1. Photochemical approaches enabling C(*sp*²)-F borylation. (A) Direct cleavage of the C-F bonds using an UV-C light source. (B) Borylation of C-F bonds under Rh/Ni dual-metal catalysis. (C) Ir-catalyzed C-F borylation. (D) C-F bond photoactivation using thiolate catalyst. (E) A versatile borylation strategy for the photoinduced activation of robust carbon-heteroatom bonds in the absence of transition metals and catalysts.





Scheme 2. Substrate scope for the borylation reactions.

^aIsolation conditions: **a** (0.1 mmol), B₂pin₂ (0.2 mmol), and CsF (0.2 mmol) in the presence of 1 mL of DMSO under 385 nm LED (2.2 W) light irradiation at 60 °C under N₂ atmosphere for 16 h. Reported isolated yields obtained by combining 5 parallel reactions.

^bThe reaction was conducted at 25 °C. ^cTetramethylammonium fluoride (Me₄NF) was used instead of CsF.

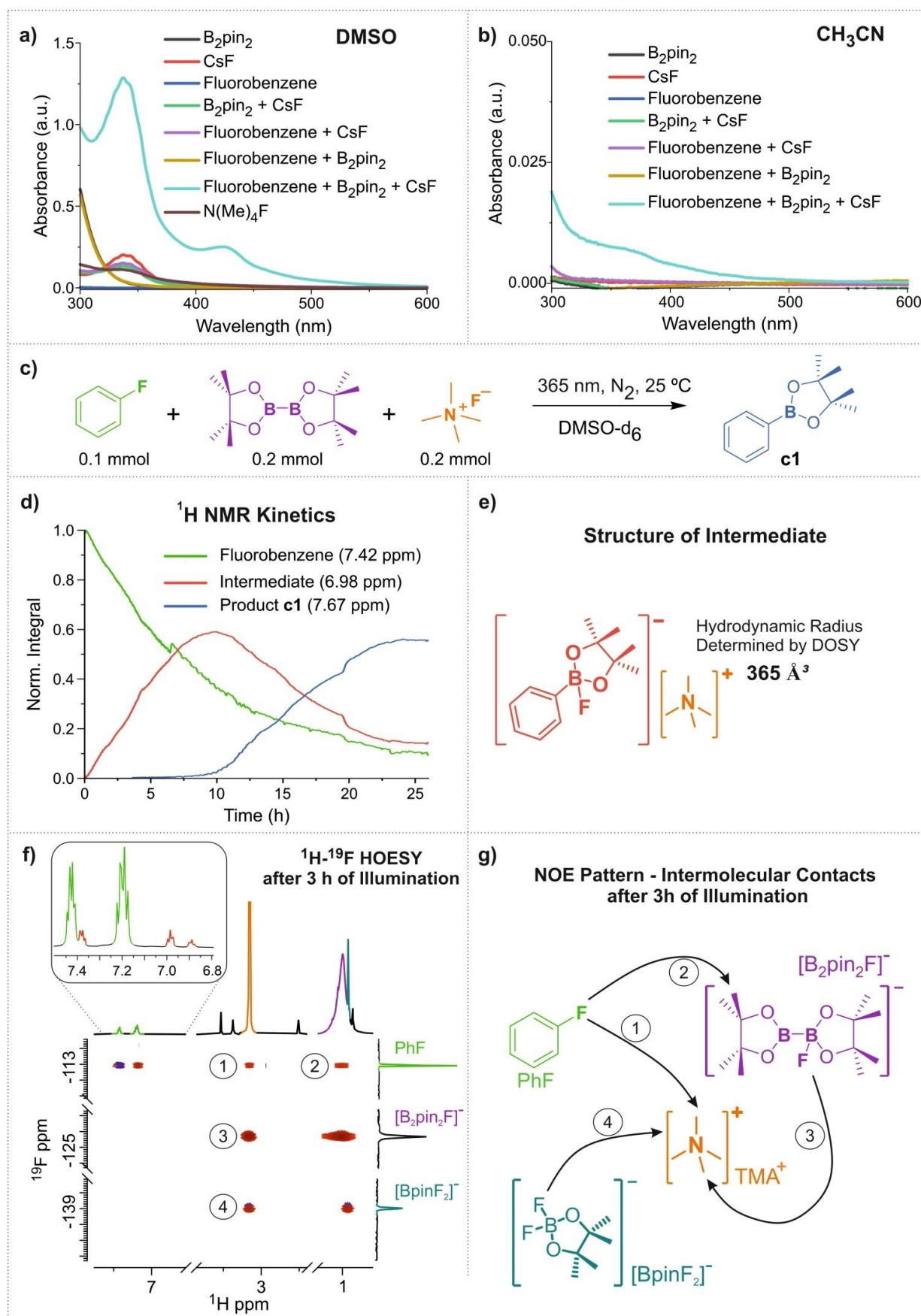
quenched the reaction (Table S1, entry 6). The use of longer wavelength light sources resulted in lower product yields (Table S4).

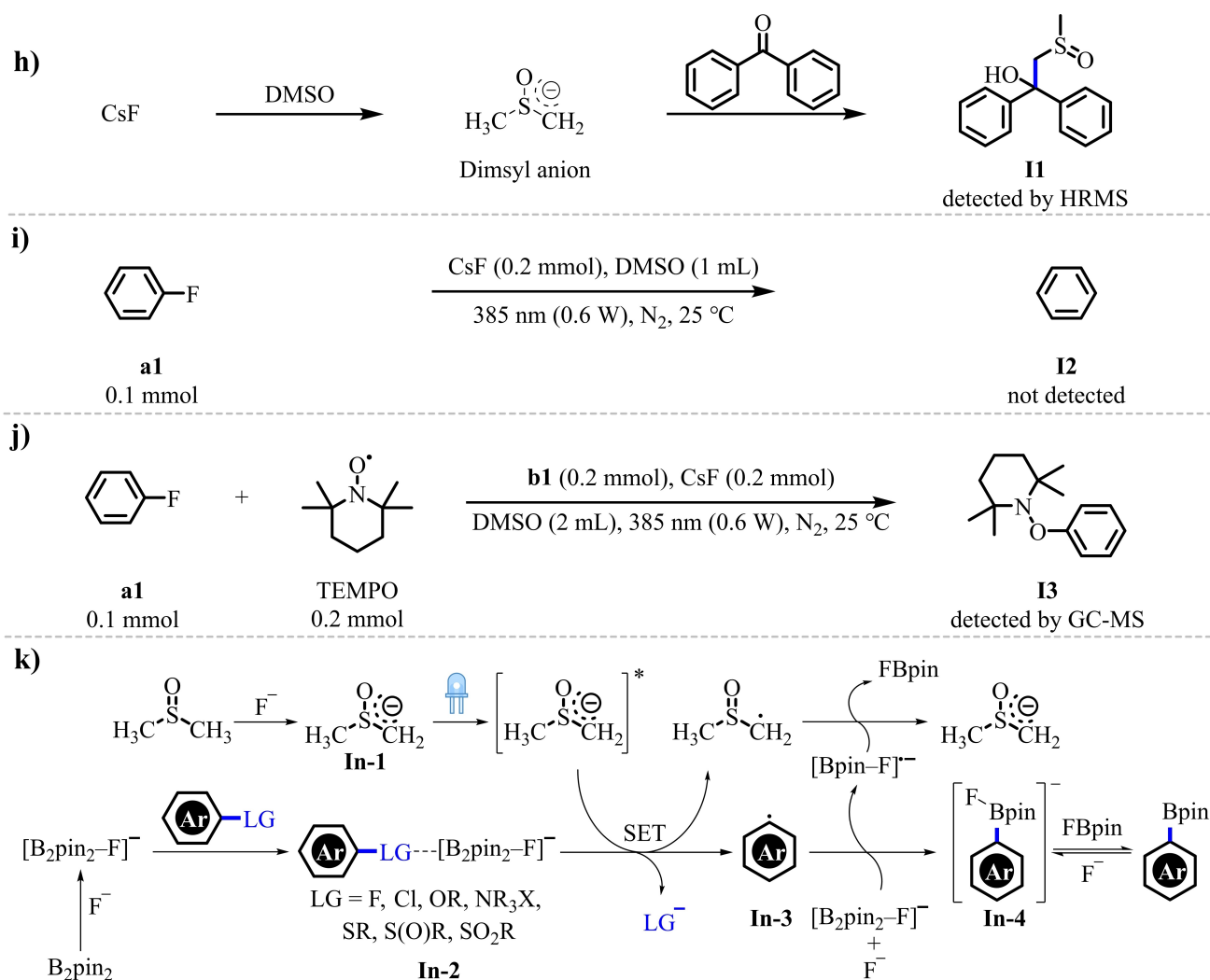
After obtaining the optimal reaction conditions, we investigated the compatibility of our methodology with diverse aryl fluorides (Scheme 2, **a1**–**a16**). Apart from electron-donating groups such as methyl (**a2**–**a4**), ethyl (**a5**), methoxy (**a6**), and hydroxy (**a7**), the introduction of alkyl alcohol (**a8**) and alkene (**a9**) substituents also led to the successful synthesis of the desired aryl boronic esters under standard reaction conditions. In addition, phenyl (**a10**), *t*-butoxycarbonyl-protected alkylamine substituent (**a11**), amide-protected alkyl substituent (**a12**), and *t*-butoxycarbonylamide (**a13**) did not impede the smooth progression of the reaction. Electron-deficient aryl ethers (**a14**), fluorobenzenes (**a15**) containing electron-withdrawing groups, and 2-fluoro-9H-fluorene (**a16**) were also well accommodated under the reaction conditions.

We effectively implemented this strategy for the activation of C(sp²)-O bonds (**a17**–**a25**). *tert*-Butyl phenyl carbonate compounds containing various substituents, including methyl (**a18**–**a20**), ethyl (**a21**), *tert*-butyl (**a22**), and methoxy (**a23**) groups, undergo C(sp²)-O bonds cleavage under the optimized conditions, leading to the generation of the target products. The use of a benzodioxole skeleton (**a24**) is also effective in borylation reactions. The trifluoromethanesulfonate moiety (**a25**) is an effective leaving group in the transformation.

Chlorobenzene compounds containing cyano (**a26**), ester (**a27**), ketone (**a28**), and pyrrole (**a29**) functionalities were effectively borylated. Naphthalene (**a30**) and indole (**a31**) chlorides convert smoothly in the reaction.

Several sulfur-containing aromatic compounds were reacted under the optimized conditions. Thioanisole derivatives (**a32**–**a35**) and aryl disulfides (**a36**, **a37**) give C(sp²)-B bonds. The method converts also





Scheme 3. Mechanistic studies. (a) UV-vis absorption spectra of reaction components in DMSO. (b) UV-vis absorption spectra of reaction components in CH_3CN . (c) Reaction system studied by *in situ* NMR. (d) ^1H NMR monitoring shows the formation of an intermediate. (e) The structure of the intermediate as confirmed by ^1H and DOSY NMR. (f) ^1H - ^{19}F HOESY of the reaction mixture after 3 h of illumination. (g) NOE Pattern observed in the reaction mixture. (h) Trapping of dimsyl anion with benzophenone. (i) The reaction doesn't proceed in the absence of B_2pin_2 . (j) Trapping of phenyl radical with TEMPO. (k) Proposed reaction mechanism.

sulfinyl (**a38**) and sulfonyl groups (**a39–a49**) into the corresponding borylated compounds. Notably, drug molecules and intermediates such as antibacterial sulfanilamide (**a45**) and anti-infective dapsone (**a46**) are also compatible. Furthermore, $\text{C}(\text{sp}^2)\text{-Br}$ (**a50**) and $\text{C}(\text{sp}^2)\text{-I}$ (**a51**) bonds also underwent efficient borylation under the optimized conditions. The efficient borylation of phenyltrimethylammonium chloride (**a52**) is also within the scope of compatibility of this strategy. However, nitrobenzene (**a53**) and aniline derivatives (**a54**) showed resistance to the reaction conditions.

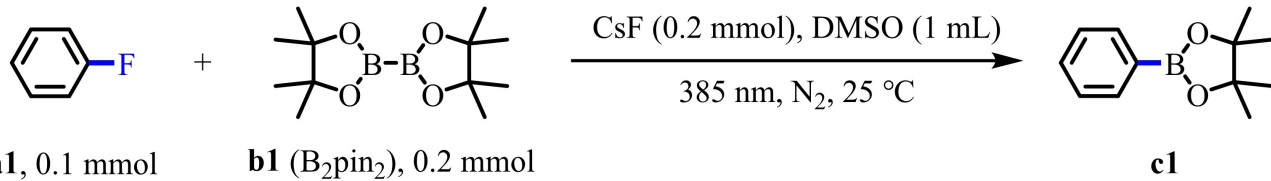
To improve the practicality of our approach, we tested the direct coupling of the borylated products without isolation, resulting in a carbon–heteroatom

borylation/Suzuki-Miyaura cross-coupling sequence and the effective synthesis of the $\text{C}(\text{sp}^2)\text{-C}(\text{sp}^2)$ coupling products (**d1–d5**).

Using a flow photochemical system, the reaction of fluorobenzene to aryl boronic ester was performed on a larger scale yielding 0.8 g of product **c1** (see SI section II for details).

Investigation of the Reaction Mechanism

To gain insight into the mechanism of the photo-induced borylation of carbon–heteroatom bonds, several spectroscopic experiments were performed. Initially, UV-vis spectra of different combinations of reagents were recorded. The addition of CsF to DMSO

Table 1. Control experiments for the reaction of **a1** with **b1**.^[a]


Entry	Deviations from Optimized Conditions	Yield of c1
1	None	90%
2	No CsF	n.d.
3	No light, 25 °C	n.d.
4	No light, 60 °C	n.d.
5	air instead of N ₂	< 1%
6	CH ₃ CN instead of DMSO	< 1%
7	DMF instead of DMSO	< 1%
8	DMA instead of DMSO	< 1%
9	DCM instead of DMSO	< 1%
10	THF instead of DMSO	< 1%

^[a] Optimized conditions: compounds **a1** (0.1 mmol), **b1** (0.2 mmol), and CsF (0.2 mmol) in the presence of 1 mL of DMSO under 385 nm LED (0.6 W) light irradiation at 25 °C under N₂ atmosphere for 16 h. Yields were determined by GC-MS analysis with n-dodecane as an internal standard and are the average of two runs. n.d., the product was not detected.

resulted in absorption above 340 nm, whereas no absorption is detected above 300 nm when CsF is added to CH₃CN (Scheme 3a, b and Figures S1, S2). It has been reported that DMSO can react with different bases to deprotonate and form the dimsyl anion, which displays absorption above 340 nm,^[87] closely resembling our experimental results. Subsequently, we added different bases to DMSO, demonstrating nearly identical absorption spectra (Scheme 3a and Figure S1), confirming the presence of the dimsyl anion. The combination of fluorobenzene with CsF or B₂pin₂ individually did not result in any change from the spectra of the individual compounds, indicating that fluorobenzene does not interact with either of them. However, a combination of CsF and B₂pin₂ showed a new absorption band in the visible region, which appears as well when CsF, B₂pin₂ and fluorobenzene are mixed. Intrigued by this observation, we employed a 451 nm light source, emitting near the newly formed absorption band, to conduct the standard reaction and monitor its progress at different time intervals (Table S4, entries 3–5). It was observed that the reaction essentially did not proceed, demonstrating that the light absorption associated with the new absorption band does not dictate the progress of the reaction.

Additionally, the UV-vis spectra of different reagent combinations in acetonitrile (Scheme 3b and Figure S2) showed that a weak absorption appeared only when CsF, fluorobenzene, and B₂pin₂ were mixed, confirming the presence of interactions in the system. However, we didn't explore further these interactions, since the reaction was not proceeding under these conditions.

B₂pin₂ can react with various bases to form anionic *sp*²–*sp*³ diboron compounds, including CsF and Me₄NF.^[48,50,85,86] The conclusion has been substantiated by our NMR studies, observing the characteristic resonance of [FB₂pin₂][−] at approximately 9 ppm in the ¹¹B NMR (Figures S3–S6, Table S8). These NMR spectra indicated that, in the absence of irradiation, the standard reaction system predominantly undergoes the reaction between B₂pin₂ and the base.

Subsequently, *in situ* NMR studies^[88] were conducted on the model reaction system (Scheme 3c), involving the photochemical reaction of fluorobenzene with B₂pin₂ in the presence of Me₄NF in DMSO-*d*₆. Due to the limited solubility of CsF in DMSO and the comparable reaction outcomes between Me₄NF and CsF in the standard reaction (Table S3, entry 11), Me₄NF was selected as a substitute for the NMR investigation.

The kinetics of the model reaction were tracked in real-time using ¹H NMR over 26 hours, as depicted in Scheme 3d and Figure S7. As fluorobenzene, the starting material, gradually depleted, a new set of signals rose and intensified, reaching their maximum concentration at 10 hours of illumination.

These signals are attributed to an intermediate, followed by gradual attenuation, which coincided with the increase in signals corresponding to the formation of product **c1** after 10 hours of reaction, indicating the correlation between the generated new compound and the product.

Diffusion-ordered spectroscopy (DOSY) studies (Figure S9, Table S9) revealed that the intermediate compound is an adduct between compound **c1** and

fluoride (fluorinated arylboronic acid ester anion), [PhBpinF][−] (Scheme 3e). Comparison of the ¹H and ¹⁹F NMR spectra of a 1:1 mixture of **c1** and the base with those of the reaction system (Figures S10 and S11) demonstrated matching chemical shifts with the structure attributed as intermediate, confirming this inference. Based on the observed data, it suggests a subsequent defluorination process of the intermediate after 10 h of reaction.

In the ¹H-¹⁹F HOESY NMR study of the reaction mixture after 3 hours of illumination, an interaction between the fluorine atom of fluorobenzene and the protons of [B₂pin₂F][−] was observed (Scheme 3f and g), confirming the dual role of B₂pin₂ as both a borylating agent and in substrate activation.

A benzophenone trapping reaction was utilized to demonstrate the existence of the dimsyl anion, resulting in the formation of 2-(methylsulfinyl)-1,1-diphenylethan-1-ol (**II**).^[87,89] We added benzophenone to the solution of CsF in DMSO and successfully detected the presence of **II** using HRMS (Scheme 3h and Figure S13), further confirming that CsF can deprotonate DMSO to generate the dimsyl anion.

A control experiment proved that without B₂pin₂, fluorobenzene did not react and benzene was not produced (as shown in Scheme 3i). This demonstrates that the photoexcited dimsyl anion is not able to break the C–F bond of fluorobenzene by itself and that B₂pin₂ plays a crucial role in this process.

After adding TEMPO to the standard reaction system, the reaction progress was almost completely inhibited. In addition, the intermediate phenyl radical captured by TEMPO was detected by GC-MS (Scheme 3j and Figure S14), confirming that the reaction proceeds via a radical process.

In the GC-MS analysis (Figure S15) conducted directly without any workup after the completion of the standard reaction, compounds BpinOBpin and dimethyl sulfide were detected. The oxygen atom of BpinOBpin is expected to originate from the active intermediate of DMSO.^[90] In addition, compound CD₃-Bpin was detected by GC-MS when DMSO-d₆ was used as the solvent (Figure S16). These results demonstrate that the subsequent decomposition process of the active intermediate in DMSO is inevitable. This could explain why catalytic amounts of DMSO, as confirmed in our control experiments (Table S2, entry 8), cannot drive the reaction to completion.

Based on these investigations, a plausible mechanism for the photoinduced borylation of carbon–heteroatom bonds is proposed (Scheme 3k and Figure S17). Firstly, the base CsF reacts with DMSO to generate the dimsyl anion (**In-1**). Simultaneously, CsF can form anionic *sp*²–*sp*³ diboron compounds [FB₂pin₂][−] with B₂pin₂, which can interact with and activate reactants bearing leaving groups (**In-2**). Under light irradiation, the excited dimsyl anion undergoes single-electron transfer with activated

aromatic compounds, accompanied by the departure of the leaving group anion and the formation of an aryl radical (**In-3**). The aryl radical, in the presence of [FB₂pin₂][−] and F[−], generates a fluorinated aryl boronic ester anionic compound (**In-4**). This anion accumulates in the early development of the reaction, and then dissociates to yield the desired neutral ester. We speculate that the reason for this is the formation of FBpin in the reaction: FBpin radical anion is formed as a by-product of the coupling of the phenyl radical to [B₂pin₂F][−] and is subsequently oxidized to the neutral FBpin compound. Then, it coordinates the excess of fluoride present in the reaction medium, thus generating the anion [F₂Bpin][−].^[91] As the reaction progresses, the amount of free fluoride decreases; as a result, FBpin, displaying a higher Lewis acidity than ArBpin, removes the fluoride from [ArBpinF][−], restoring the neutral ester.

Conclusion

In conclusion, the photochemical borylation reaction of inert carbon–heteroatom bonds has been achieved under simple and mild reaction conditions. Photocatalysts or transition metals are not required. The experimental results demonstrate that the key to activating strong carbon–heteroatom bonds lies in the reaction of DMSO with the base to generate the dimsyl anion, as well as the pre-activation of leaving groups by the anionic *sp*²–*sp*³ diboron compound. The application of the method in synthesis has been demonstrated by a borylation/Suzuki-Miyaura coupling reaction sequence and its use in continuous-flow photochemical synthesis, providing a straightforward and effective approach to the construction of arylboronic esters.

Experimental Section

Procedures for the Optimization of the Reaction Conditions

Unless specified otherwise, a mixture of B₂pin₂ (0.2 mmol) and base (0.2 mmol) was added to an oven-dried 5 mL snap vial equipped with a magnetic stirring bar. Then 1 mL solvent (DMSO or other organic solvents) was added to the vial by syringe. Fluorobenzene (0.1 mmol) was subsequently added into the reaction system by syringe. The solution was then bubbled with N₂ for 3 min. Then, the cap was sealed with parafilm. The reaction mixture was stirred and irradiated with a 385 nm (0.6 W or 2.2 W) LED (for the screening of the light sources, 0.6 W of 365 nm, 385 nm, 400 nm, 451 nm LEDs were used) at 25 °C (for the control experiments, reactions were also conducted under 60 °C) for 16 h. Saturated brine (2 mL) was added to the system and diluted with ethyl acetate (2 mL), and then filtered through a plug of celite (Ø 3 mm×8 mm). After addition of *n*-dodecane (0.2 mmol) as an internal standard for calibration, the product yield was determined by GC-MS.

Procedures for the Isolation of the Final Products

Unless specified otherwise, five parallel reactions of B_2pin_2 (0.2 mmol) and CsF (0.2 mmol) were added to five oven-dried 5 mL snap vials equipped with magnetic stirring bars, separately. Then 1 mL DMSO was added to each vial by syringe. Compound **a** (0.1 mmol) was subsequently added into the reaction system. The solution was then bubbled with N_2 for 3 min. Then, the cap was sealed with parafilm. The reaction mixture was irradiated with a 385 nm LED (2.2 W) at 60 °C for 16 h (to optimize and adjust specific reaction conditions, refer to the substrate scope section in the main text, where deviations from the standard procedure are described). Saturated brine (3 mL) was then added to each reaction system and extracted with ethyl acetate (2 mL \times 3). The combined organic phase was then dried over sodium sulfate and concentrated under vacuum. The residue was purified by silica gel flash chromatography to give the desired product.

Acknowledgments

This work was supported by the Deutsche Forschungsgemeinschaft [DFG (German Science Foundation) grant TRR 325-444632635]. W.S. is funded by DFG grant RTG 2620, "Ion Pair Effects in Molecular Reactivity" project 426795949). We thank R. Vasold for assistance in GC-MS measurements, J. Zach for technical assistance and A. Antonov for the critical discussion of our results.

References

- [1] C. D. Entwistle, T. B. Marder, *Angew. Chem. Int. Ed.* **2002**, *41*, 2927–2931.
- [2] C. D. Entwistle, T. B. Marder, *Chem. Mater.* **2004**, *16*, 4574–4585.
- [3] I. A. I. Mkhaliid, J. H. Barnard, T. B. Marder, J. M. Murphy, J. F. Hartwig, *Chem. Rev.* **2010**, *110*, 890–931.
- [4] F. Jakle, *Chem. Rev.* **2010**, *110*, 3985–4022.
- [5] D. G. Hall, *Boronic Acids: Preparation and Applications in Organic Synthesis Medicine and Materials*, 2nd ed., Wiley-VCH, Weinheim **2011**.
- [6] F. Issa, M. Kassiou, L. M. Rendina, *Chem. Rev.* **2011**, *111*, 5701–5722.
- [7] V. M. Dembitsky, A. A. Al Quntar, M. Srebnik, *Chem. Rev.* **2011**, *111*, 209–237.
- [8] R. Smoum, A. Rubinstein, V. M. Dembitsky, M. Srebnik, *Chem. Rev.* **2012**, *112*, 4156–4220.
- [9] A. Lorbach, A. Hubner, M. Wagner, *Dalton Trans.* **2012**, *41*, 6048–6063.
- [10] A. R. Martin, J. J. Vasseur, M. Smietana, *Chem. Soc. Rev.* **2013**, *42*, 5684–5713.
- [11] E. C. Neeve, S. J. Geier, I. A. I. Mkhaliid, S. A. Westcott, T. B. Marder, *Chem. Rev.* **2016**, *116*, 9091–9161.
- [12] A. B. Cuenca, R. Shishido, H. Ito, E. Fernández, *Chem. Soc. Rev.* **2017**, *46*, 415–430.
- [13] I. F. Yu, J. W. Wilson, J. F. Hartwig, *Chem. Rev.* **2023**, *123*, 11619–11663.
- [14] L. Ji, S. Griesbeck, T. B. Marder, *Chem. Sci.* **2017**, *8*, 846–863.
- [15] E. Khotinsky, M. Melamed, *Ber. Dtsch. Chem. Ges.* **1909**, *42*, 3090–3096.
- [16] R. L. Letsinger, I. H. Skoog, *J. Org. Chem.* **1953**, *18*, 895–897.
- [17] S. K. Bose, L. Mao, L. Kuehn, U. Radius, J. Nekvinda, W. L. Santos, S. A. Westcott, P. G. Steel, T. B. Marder, *Chem. Rev.* **2021**, *121*, 13238–13341.
- [18] J. Hu, M. Fenger, Z. Shi, T. B. Marder, *Chem. Soc. Rev.* **2021**, *50*, 13129–13188.
- [19] Z.-H. Shang, J. Pan, Z. Wang, Z.-X. Zhang, J. Wu, *Eur. J. Org. Chem.* **2023**, *26*, e202201379.
- [20] W. K. Chow, O. Y. Yuen, P. Y. Choy, C. M. So, C. P. Lau, W. T. Wong, F. Y. Kwong, *RSC Adv.* **2013**, *3*, 12518–12539.
- [21] J. Zhou, M. W. Kuntze-Fechner, R. Bertermann, U. S. D. Paul, J. H. J. Berthel, A. Friedrich, Z. Du, T. B. Marder, U. Radius, *J. Am. Chem. Soc.* **2016**, *138*, 5250–5253.
- [22] X.-W. Liu, J. Echavarren, C. Zarate, R. Martin, *J. Am. Chem. Soc.* **2015**, *137*, 12470–12473.
- [23] T. Niwa, H. Ochiai, Y. Watanabe, T. Hosoya, *J. Am. Chem. Soc.* **2015**, *137*, 14313–14318.
- [24] M. Sun, M. Tao, L. Zhao, W. Li, Z. Liu, C.-Y. He, Z. Feng, *Org. Chem. Front.* **2021**, *8*, 5322–5327.
- [25] S. K. Bose, A. Deibenberger, A. Eichhorn, P. G. Steel, Z. Lin, T. B. Marder, *Angew. Chem. Int. Ed.* **2015**, *54*, 11843–11847.
- [26] Q. Liu, L. Zhang, F. Mo, *Acta Chim. Sinica* **2020**, *78*, 1297–1308.
- [27] M. Teltewskoi, J. A. Panetier, S. A. Macgregor, T. Braun, *Angew. Chem. Int. Ed.* **2010**, *49*, 3947–3951.
- [28] W.-H. Guo, Q.-Q. Min, J.-W. Gu, X. Zhang, *Angew. Chem. Int. Ed.* **2015**, *54*, 9075–9078.
- [29] R. J. Lindup, T. B. Marder, R. N. Perutz, A. C. Whitwood, *Chem. Commun.* **2007**, *35*, 3664–3666.
- [30] R. Seki, N. Hara, T. Saito, Y. Nakao, *J. Am. Chem. Soc.* **2021**, *143*, 6388–6394.
- [31] L. Luo, S. Tang, J. Wu, S. Jin, H. Zhang, *Chem. Rec.* **2023**, *23*, e202300023.
- [32] C. Zarate, R. Manzano, R. Martin, *J. Am. Chem. Soc.* **2015**, *137*, 6754–6757.
- [33] K. C. Morris, S. E. Wright, G. F. Meyer, T. B. Clark, *J. Org. Chem.* **2020**, *85*, 14795–14801.
- [34] F. W. Friese, A. Studer, *Chem. Sci.* **2019**, *10*, 8503–8518.
- [35] M. Wang, Z. Shi, *Chem. Rev.* **2020**, *120*, 7348–7398.
- [36] G. Yan, D. Huang, X. Wu, *Adv. Synth. Catal.* **2018**, *360*, 1040–1053.
- [37] Y. Ma, Y. Pang, S. Chhabra, E. J. Reijerse, A. Schnegg, J. Niski, M. Leutzsch, J. Cornella, *Chem. Eur. J.* **2020**, *26*, 3738–3743.
- [38] J. Wang, M. Shang, H. Lundberg, K. S. Feu, S. J. Hecker, T. Qin, D. G. Blackmond, P. S. Baran, *ACS Catal.* **2018**, *8*, 9537–9542.
- [39] K. Kubota, H. Iwamoto, H. Ito, *Org. Biomol. Chem.* **2017**, *15*, 285–300.
- [40] R. Farzana, P. V. Saranya, A. Gopinathan, *J. Organomet. Chem.* **2023**, *983*, 122549–122569.
- [41] L. Kuehn, L. Zapf, L. Werner, M. Stang, S. Würtemberger-Pietsch, I. Krummenacher, H. Braunschweig, E.

- Lacôte, T. B. Marder, U. Radius, *Chem. Sci.* **2022**, *13*, 8321–8333.
- [42] L. Kuehn, D. G. Jammal, K. Lubitz, T. B. Marder, U. Radius, *Chem. Eur. J.* **2019**, *25*, 9514–9521.
- [43] L. Kuehn, M. Huang, U. Radius, T. B. Marder, *Org. Biomol. Chem.* **2019**, *17*, 6601–6606.
- [44] Y. P. Budiman, S. Lorenzen, Z. Liu, U. Radius, T. B. Marder, *Chem. Eur. J.* **2021**, *27*, 3869–3874.
- [45] M. Huang, Z. Wu, J. Krebs, A. Friedrich, X. Luo, S. A. Westcott, U. Radius, T. B. Marder, *Chem. Eur. J.* **2021**, *27*, 8149–8158.
- [46] M. Huang, M. Tang, J. Hu, S. A. Westcott, U. Radius, T. B. Marder, *Chem. Commun.* **2022**, *58*, 395–398.
- [47] Y.-M. Tian, X.-N. Guo, H. Braunschweig, U. Radius, T. B. Marder, *Chem. Rev.* **2021**, *121*, 3561–3597.
- [48] Y. M. Tian, X. N. Guo, I. Krummenacher, Z. Wu, J. Nitsch, H. Braunschweig, U. Radius, T. B. Marder, *J. Am. Chem. Soc.* **2020**, *142*, 18231–18242.
- [49] G. Ma, C. Chen, S. Talukdar, X. Zhao, C. Lei, H. Gong, *Chem. Commun.* **2020**, *56*, 10219–10222.
- [50] J. Xu, J. Cao, X. Wu, H. Wang, X. Yang, X. Tang, R. W. Toh, R. Zhou, E. K. L. Yeow, J. Wu, *J. Am. Chem. Soc.* **2021**, *143*, 13266–13273.
- [51] C. Shu, A. Noble, V. K. Aggarwal, *Nature* **2020**, *586*, 714–719.
- [52] A. Fawcett, J. Pradeilles, Y. Wang, T. Mutsuga, E. L. Myers, V. K. Aggarwal, *Science* **2017**, *357*, 283–286.
- [53] Q. Wei, Y. Lee, W. Liang, X. Chen, B.-S. Mu, X.-Y. Cui, W. Wu, S. Bai, Z. Liu, *Nat. Commun.* **2022**, *13*, 7112–7120.
- [54] S. Jin, H. T. Dang, G. C. Haug, R. He, V. D. Nguyen, V. T. Nguyen, H. D. Arman, K. S. Schanze, O. V. Larionov, *J. Am. Chem. Soc.* **2020**, *142*, 1603–1613.
- [55] M. Li, S. Liu, H. Bao, Q. Li, Y.-H. Deng, T.-Y. Sun, L. Wang, *Chem. Sci.* **2022**, *13*, 4909–4914.
- [56] A. Noble, R. S. Mega, D. Pflästerer, E. L. Myers, V. K. Aggarwal, *Angew. Chem. Int. Ed.* **2018**, *57*, 2155–2159.
- [57] L. Pan, M. V. Cooke, A. Spencer, S. Laulhé, *Adv. Synth. Catal.* **2022**, *364*, 420–425.
- [58] L. Pan, M. M. Deckert, M. V. Cooke, A. R. Bleeke, S. Laulhé, *Org. Lett.* **2022**, *24*, 6466–6471.
- [59] L. Zhang, L. Jiao, *Chem. Sci.* **2018**, *9*, 2711–2722.
- [60] L. Zhang, L. Jiao, *J. Am. Chem. Soc.* **2019**, *141*, 9124–9128.
- [61] L. Zhang, Z.-Q. Wu, L. Jiao, *Angew. Chem. Int. Ed.* **2020**, *59*, 2095–2099.
- [62] A. M. Mfuh, J. D. Doyle, B. Chhetri, H. D. Arman, O. V. Larionov, *J. Am. Chem. Soc.* **2016**, *138*, 2985–2988.
- [63] Y.-M. Tian, X.-N. Guo, M. W. Kuntze-Fechner, I. Krummenacher, H. Braunschweig, U. Radius, A. Steffen, T. B. Marder, *J. Am. Chem. Soc.* **2018**, *140*, 17612–17623.
- [64] P.-J. Xia, Z.-P. Ye, Y.-Z. Hu, J.-A. Xiao, K. Chen, H.-Y. Xiang, X.-Q. Chen, H. Yang, *Org. Lett.* **2020**, *22*, 1742–1747.
- [65] S. Wang, H. Wang, B. König, *Chem* **2021**, *7*, 1653–1665.
- [66] B. Yadagiri, K. Daipule, S. P. Singh, *Asian J. Org. Chem.* **2021**, *10*, 7–37.
- [67] Y. Cheng, C. Mück-Lichtenfeld, A. Studer, *Angew. Chem. Int. Ed.* **2018**, *57*, 16832–16836.
- [68] K. Matsuo, E. Yamaguchi, A. Itoh, *J. Org. Chem.* **2023**, *88*, 6176–6181.
- [69] T. Biremond, M. Riomet, P. Jubault, T. Poisson, *Chem. Rec.* **2023**, *23*, e202300172.
- [70] M. Jiang, H. Yang, H. Fu, *Org. Lett.* **2016**, *18*, 5248–5251.
- [71] J. Yu, L. Zhang, G. Yan, *Adv. Synth. Catal.* **2012**, *354*, 2625–2628.
- [72] Y. Qiao, Q. Yang, E. J. Schelter, *Angew. Chem. Int. Ed.* **2018**, *57*, 10999–11003.
- [73] S. Ahammed, S. Nandi, D. Kundu, B. C. Ranu, *Tetrahedron Lett.* **2016**, *57*, 1551–1554.
- [74] T. Lei, S.-M. Wei, K. Feng, B. Chen, C.-H. Tung, L.-Z. Wu, *ChemSusChem* **2020**, *13*, 1715–1719.
- [75] K. Chen, S. Zhang, P. He, P. Li, *Chem. Sci.* **2016**, *7*, 3676–3680.
- [76] L. Du, L. Sun, H. Zhang, *Chem. Commun.* **2022**, *58*, 1716–1719.
- [77] L. Candish, M. Teders, F. Glorius, *J. Am. Chem. Soc.* **2017**, *139*, 7440–7443.
- [78] W. Liu, X. Yang, Y. Gao, C.-J. Li, *J. Am. Chem. Soc.* **2017**, *139*, 8621–8627.
- [79] A. Nitelet, D. Thevenet, B. Schiavi, C. Hardouin, J. Fournier, R. Tamion, X. Pannecoucke, P. Jubault, T. Poisson, *Chem. Eur. J.* **2019**, *25*, 3262–3266.
- [80] J. Wu, R. M. Bär, L. Guo, A. Noble, V. K. Aggarwal, *Angew. Chem. Int. Ed.* **2019**, *58*, 18830–18834.
- [81] D. Mazzarella, G. Magagnano, B. Schweitzer-Chaput, P. Melchiorre, *ACS Catal.* **2019**, *9*, 5876–5880.
- [82] K. Chen, M. S. Cheung, Z. Lin, P. Li, *Org. Chem. Front.* **2016**, *3*, 875–879.
- [83] C. Huang, J. Feng, R. Ma, S. Fang, T. Lu, W. Tang, D. Du, J. Gao, *Org. Lett.* **2019**, *21*, 9688–9692.
- [84] H. Wang, J.-F. Zhao, X.-L. Zhu, Q.-Q. Tian, W. He, *Org. Lett.* **2023**, *25*, 6485–6489.
- [85] S. Pietsch, E. C. Neeve, D. C. Apperley, R. Bertermann, F. Mo, D. Qiu, M. S. Cheung, L. Dang, J. Wang, U. Radius, Z. Lin, C. Kleeberg, T. B. Marder, *Chem. Eur. J.* **2015**, *21*, 7082–7099.
- [86] R. D. Dewhurst, E. C. Neeve, H. Braunschweig, T. B. Marder, *Chem. Commun.* **2015**, *51*, 9594–9607.
- [87] M. E. Budén, J. I. Bardagí, M. Puiatti, R. A. Rossi, *J. Org. Chem.* **2017**, *82*, 8325–8333.
- [88] C. Feldmeier, H. Bartling, E. Riedle, R. M. Gschwind, *J. Magn. Reson.* **2013**, *232*, 39–44.
- [89] P. Speers, K. E. Laidig, A. Streitwieser, *J. Am. Chem. Soc.* **1994**, *116*, 9257–9261.
- [90] J. Li, H. Wang, Z. Qiu, C.-Y. Huang, C.-J. Li, *J. Am. Chem. Soc.* **2020**, *142*, 13011–13020.
- [91] L. Kuehn, M. Stang, S. Würtemberger-Pietsch, A. Friedrich, H. Schneider, U. Radius, T. B. Marder, *Faraday Discuss.* **2019**, *220*, 350–363.

RESEARCH ARTICLE

Photoinduced Radical Borylation of Robust Carbon–Heteroatom Bonds

Adv. Synth. Catal. **2024**, *366*, 1–11

 Y.-M. Tian, X. Pu, A. H. Sánchez, W. Silva, R. M. Gschwind, B. König*

